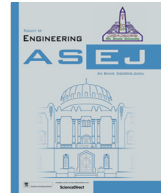




Contents lists available at ScienceDirect

Ain Shams Engineering Journal

journal homepage: [www.sciencedirect.com](http://www.sciencedirect.com)

Civil Engineering

# The effect of long-term consolidation on foundations underpinned by micropiles in soft clay

Walid El Kamash<sup>a,1,\*</sup>, Hany El Naggar<sup>b</sup>, Peter To<sup>c</sup>, Nagaratnam Sivakugan<sup>c</sup><sup>a</sup> Associate Professor, Department of Civil Engineering, Faculty of Engineering, Suez Canal University, Ismailia 41522, Egypt<sup>b</sup> Department of Civil and Resource Engineering, Dalhousie University, Nova Scotia B3H 4R2, 1360, Canada<sup>c</sup> College of Science & Engineering, James Cook University, Townsville, QLD 4811, Australia

## ARTICLE INFO

## Article history:

Received 28 December 2020

Revised 21 April 2021

Accepted 2 May 2021

Available online 20 May 2021

## Keywords:

Micropiles

Modified Cam Clay model

Consolidation settlement

Numerical model

Soft clay

Constitutive model

## ABSTRACT

So far insufficient research has been done on the long-term behavior of micropiles embedded in a clay medium, even though this has a significant influence on the expected total settlement. This paper considers a square foundation placed on a clay bed and tested under vertical loads until the clay reached its bearing capacity. Subsequently, the plate was underpinned with four micropiles, and the load test was repeated. These test data were used to validate the coupled hydraulic-mechanical three-dimensional finite difference model presented in this paper. In the numerical modelling, four different load transfer scenarios were considered to simulate different approaches to adding floors to an existing building. Consolidation periods of zero months, six months, and five years between the application of the load due to the existing building, and the application of loads due to additional storeys were considered. The six-month period represents a short-term, and the five-year period a long-term scenario. Following the first consolidation period and the application of loads representing additional storeys, a second consolidation period was implemented, such that the combined length of the two consolidation periods was five years. In this study, the results showed that the installation of micropiles immediately after the completion of existing floors is most successful in controlling the settlement of additional floors later on.

© 2021 THE AUTHORS. Published by Elsevier BV on behalf of Faculty of Engineering, Ain Shams University. This is an open access article under the CC BY-NC-ND license (<http://creativecommons.org/licenses/by-nc-nd/4.0/>).

## 1. Introduction

Soft clays exist in many countries as natural clays, and as recent deposits such as dredged material in reclaimed lands. Structures built on soft clays often experience excessive settlement and have a low load-bearing capacities. When these structures are subject to increased loads, their structural integrity may be jeopardized by settlement that exceeds acceptable limits and/or possible bearing capacity failure [1,2,3,7,4]. Increasing the height of buildings by adding additional storeys imposes greater loads on the founda-

tions, often necessitating modifications to the existing foundations. However, micropiles are used as an effective method of mitigating settlement and preventing possible bearing capacity failure. Micropiles have been used worldwide for underpinning foundations.

Micropiles are typically classified into four classes according to the grouting systems suggested by the FHWA [10]: gravity grout, pressure grout, single global postgrout and multiple repeatable postgrout, which are gravity grout, pressure grouted through the casing, primary grout placed under gravity head then pressure grouting, and primary grout placed under gravity head then high-pressure grouting. Micropile grouting is used to transmit the axial load from the steel reinforcement to the surrounding soil and to protect the steel reinforcement against corrosion.

Singh and Heine [20] performed a case study in which existing foundations were underpinned by micropiles of type B, where grout is placed via a casing under pressure. These researchers carried out full-scale load tests and found that their predicted settlements agreed well with measured settlements. Micropile laboratory model tests and field tests were carried out by Borthakur and Dey [5], Guo et al. [11], and Capatti et al. [6].

\* Corresponding author.

E-mail address: [waleedkamash@eng.suez.edu.eg](mailto:waleedkamash@eng.suez.edu.eg) (W. El Kamash).<sup>1</sup> Visiting research academic, James Cook University, Townsville, Australia.

Peer review under responsibility of Ain Shams University.



Srivastava et al. [18] performed a numerical study of micropiles by using PLAXIS 2D to analyze the stability of an excavation 18 m deep for a 3-storey basement structure.

Various experimental and theoretical approaches have been developed to analyze the load-bearing behavior of micropiles. These include the experimental centrifuge tests of Alnuaim et al. [2] and Mashhoud et al. [15], the numerical and analytical models of Zhang et al. [23], Ni et al. [16], Qian & Lu [17], and Alnuaim et al. (2015a, 2015b, 2016), and the fieldwork approaches of Han and Ye [12]. The effect of micropile configurations, focusing on improved load-bearing behavior, has also been investigated by Lizzi and Carnevale [13], Tsukada et al. [22], Seo et al. [19] and Kyung et al. [14]. Field load tests conducted by Lizzi and Carnevale [13] showed that the optimum distance between micropiles in a group configuration was 3 to 4 times the micropile diameter, with an optimum micropile length of 10 to 30 m, depending on the soil conditions. Model load tests performed by Tsukada et al. [22], Sharma et al. [21], and Kyung et al. [14] suggested that micropiles mounted at an inclination of 15° to 30° exhibited a greater compressive load-bearing efficiency than micropiles installed vertically.

El Kamash and Han [7] studied the mechanism for the transfer of loads from the superstructure to the underlying foundation underpinned by micropiles. They focused on the scenario where an existing structure is subject to additional loads. The finite difference code FLAC<sup>3D</sup> 3.0 [9] was used to simulate underpinning in the field and the soft clay was modelled as a Mohr-Coulomb material, without considering its hydraulic properties. Only short-term behavior was studied, by using undrained shear strength parameters.

In the current study presented in this paper, the model of El Kamash and Han [7] is extended with a different constitutive soil model to investigate long-term settlement due to consolidation. Here the soft clay is modelled as a Modified Cam Clay (MCC) material with appropriate parameters. To simulate the consolidation process in the soft clay, a coupled hydraulic-mechanical model is used. The objective of the current study is to investigate the effect of the consolidation period on the existing foundation, prior to adding storeys that subject the foundation to additional loads.

## 2. Numerical modeling

In order to calibrate the new constitutive soil model to study the effects of consolidation, the MCC parameters, which differ from Mohr-Coulomb parameters, were investigated and incorporated into the new model. The calibration was performed by comparing the settlements obtained from the present study with original measurements obtained from a field test, as well as numerical results from a previous study. Because of the problem's symmetry, only one-quarter of the simulation configuration was used in the analysis. In the 3D model, a radially graded mesh has also been used to surround cylindrically shipped tunnel elements and cylindrical elements. The elements were solid and had soil characteristics. The cylindrical elements were utilized to model the micropiles, while the cylindrical tunnel elements were used to generate the soil around the micropile. The mesh of the cylindrical elements of the micropile was refined. The discretization was gradually increased through the radially cylindrical elements of the surrounding soil until it reached the side boundaries. To develop the soil end-bearing reaction, the soil beneath the pile tip was modelled using radially cylindrical elements with filling. Before installing the micropiles, the radially cylindrical elements were used to model an opening on the loading plate above the natural ground for the underpinned foundation, which was then filled with radially cylindrical elements with filling to ensure connectivity between the micropiles and the foundation plate.

Fig. 1 illustrates the mesh used in the FLAC<sup>3D</sup> 3.0 [9] model. A numerical model using the Modified Cam Clay (coupled hydraulic-mechanical) approach was developed to study the long-term behavior of a concrete plate subject to loading and underpinned by micropiles [7]. As shown in Fig. 1b and 1c, the concrete plate dimensions were 1.5 m × 1.5 m in the plan view, with a thickness of 55 mm. The top 1.0 m of the topsoil was removed, and the concrete plate was treated as a highly rigid solid element.

In this study, the Modified Cam Clay represents the normally consolidated clays, where the modulus of elasticity increases due to the reduction in volume during consolidation. The problem was examined in a series of undrained and drained states. The problem was first examined in an undrained state, and then in a drained state. Under drained conditions, an iterative procedure of mechanically and hydraulically coupled numerical modelling, consisting of mechanical and hydraulic cycles, was being used. Each mechanical cycle computed stresses and deformations, while each hydraulic cycle modelled the consolidation mechanism by diffusion of excess pore water pressure through the soil. Both loops were connected using the quasi-static Biot theory (Biot [24]), with the first hydraulic loop using Darcy's law, the fluid mass balance law, and the computability law to compute pore water pressure and precise discharge. Second, the pore water pressures were fed into a mechanical loop to calculate effective stresses, which were then used to verify failure characteristics and calculate volumetric strain using the chosen constitutive model. Finally, in an iterative process based on the linear quasi-static Biot theory, the modified volumetric strain was transferred back to the new hydraulic loop to compute a new improvement in the pore water pressure (Itasca, 2005). The force balance (within a tolerance) was achieved after several cycles of alternative loops, and both pore water pressure and volumetric strain were revised. The bottom boundary was set both horizontally and vertically, while the two side boundaries were fixed horizontally but not vertically.

The input parameters, derived based on the studies of El Kamash and Han [8] and Han and Ye [12], are summarized in Table 1.

Fig. 2 shows pressure-settlement curves (in blue) for a loading-unloading cycle of a plate loading field test performed at a site in Shanghai, China. This is the same field test as that presented by Han and Ye (2006). In the test, the soil profile consisted of a lean clay layer at ground level underlain by a thick layer of fat clay, with the water table located within 1.0 m below the ground level. The total compressive strength of the lean clay determined by CU triaxial tests ranged from 70 kPa to 100 kPa. The load test data indicated that the ground yielded at an applied pressure of 89 kPa. As well as showing the measured field data and results of the present study, Fig. 2 also presents pressure-settlement results of the study by El Kamash and Han [7] which used the Mohr-Coulomb constitutive model and considered only a mechanical analysis.

The numerical analysis was based on the Modified Cam Clay (MCC) model to consider coupled hydraulic-mechanical processes. To simulate undrained conditions, fluid was set to "off". In Fig. 2, a loading-unloading cycle analysis with MCC is compared with field test measurements [12] and with the results of an analysis based on the Mohr-Coulomb (MC) constitutive model [7]. The results of the current study using MCC showed good agreement with both the test data and the results of the analysis using the Mohr-Coulomb model. This validation permitted the MCC model to be used further in the research.

In addition to the verification with the field plate load test, shown in Fig. 2, other load tests were also carried out. A plate was underpinned by micropiles with a radius of 150 mm. As illustrated in Fig. 1b, the clearance allowed by holes in the plate initially prevented a connection between the plate and the installed micropiles. The plate with micropiles was subjected to a loading-

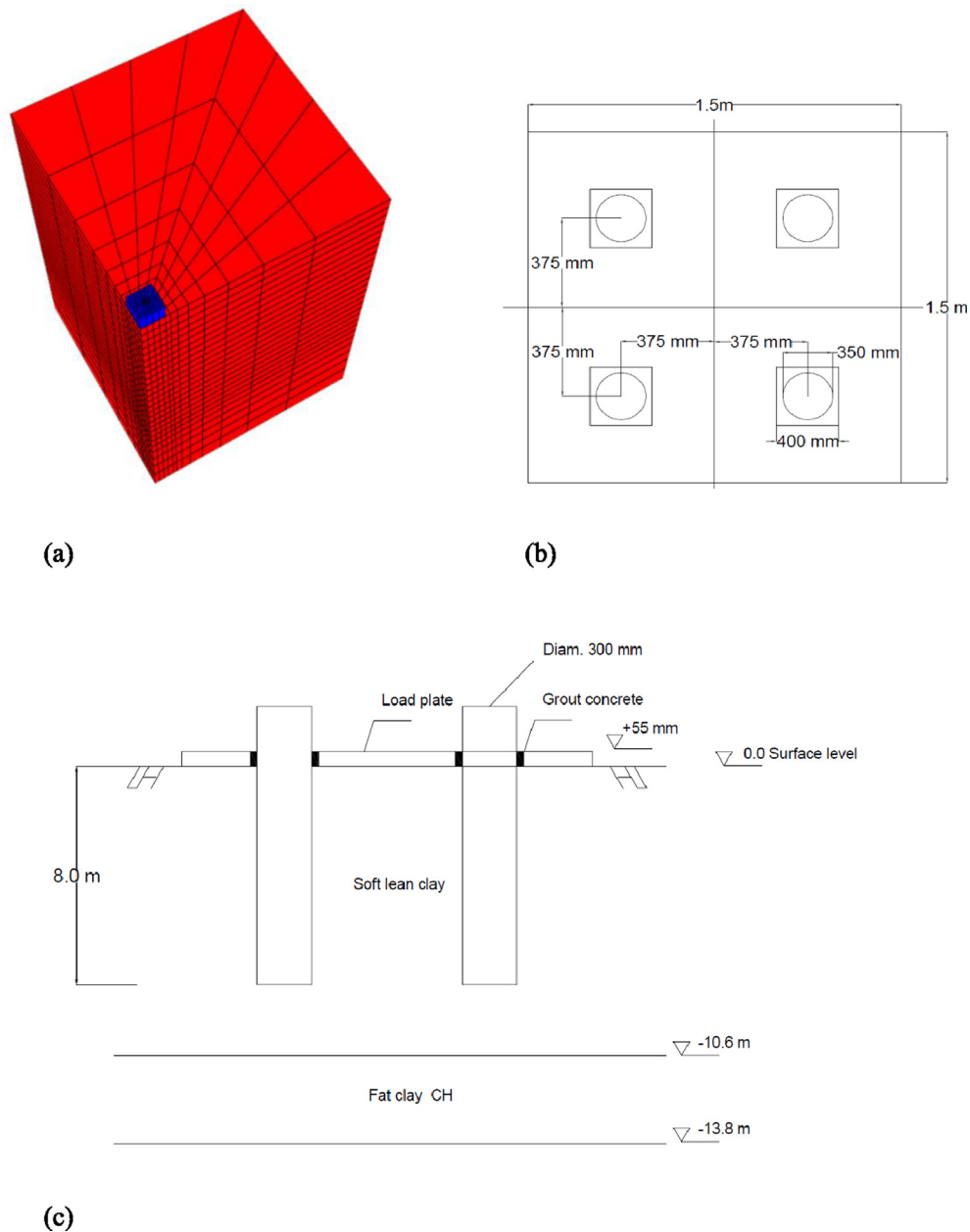


Fig. 1. The numerical model (a) Illustration of mesh used in the 3D numerical model, (b) plan view of the plate and micropiles, and (c) elevation view and soil profile (not to scale).

Table 1  
Soft clay soil property input parameters for the MCC model.

| Parameters | Slope of elastic swelling line | Slope of normal consolidation line | Friction constant | Poisson's ratio | Preconsolidation pressure kPa | Specific volume at reference pressure (1 kPa) |
|------------|--------------------------------|------------------------------------|-------------------|-----------------|-------------------------------|---|
| Symbols    | $\kappa$                       | $\lambda$                          | M                 | $\nu$           | $P_c$                         | $e_r$   |
| Values     | 0.08                           | 0.21                               | 0.877             | 0.4             | 175.6                         | 2.75  |

unloading cycle similar to that used for the plate alone. The pressure–settlement curve for the plate with micropiles is shown in Fig. 3, where the results of the simulation with the Modified Cam Clay (MCC) model are compared with measurements from field load test data presented by Han and Ye [12] as well as with results of the numerical analysis by El Kamash and Han [7] where the soft clay was simulated with the Mohr–Coulomb (MC) model. The plate was first loaded to 89 kPa, which was determined to be the applied

pressure at which the ground yielded. This simulated the first stage of loading, before yielding of the natural ground (see Fig. 3). Subsequently, the holes in the plate were filled with concrete, to guarantee a complete connection between the plate and the micropiles. The second stage of loading then began at 89 kPa and loads were increased to 280 kPa, following the loading sequence used in the field test by Han and Ye [12]. In the current study using the Modified Cam Clay model and a coupled hydraulic-mechanical tech-

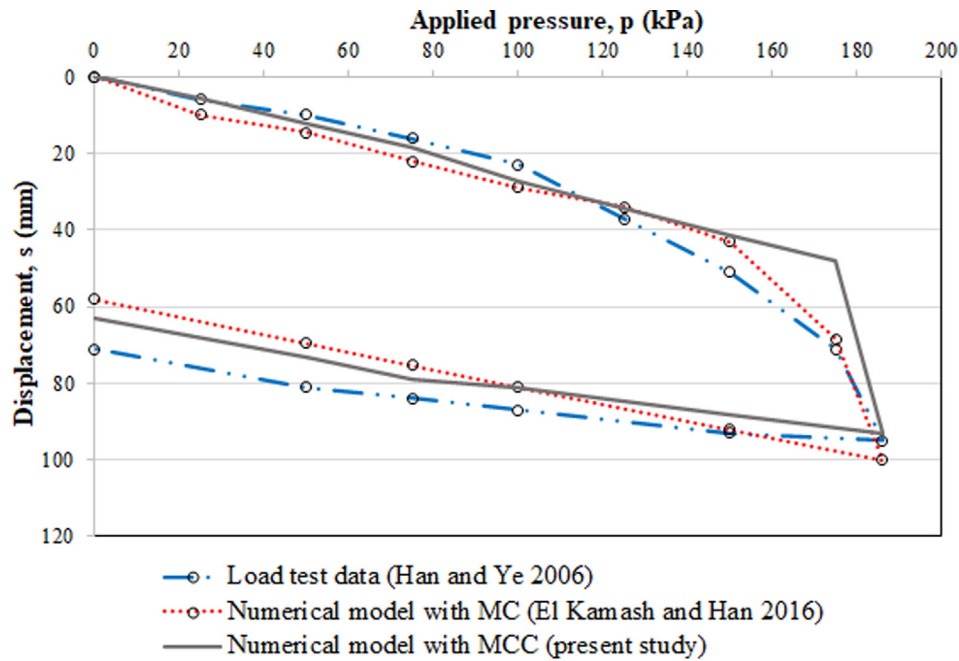


Fig. 2. Loading-unloading pressure-settlement curves, comparing the analysis using MCC with a field plate load test and with an analysis using the Mohr-Coulomb (MC) model.

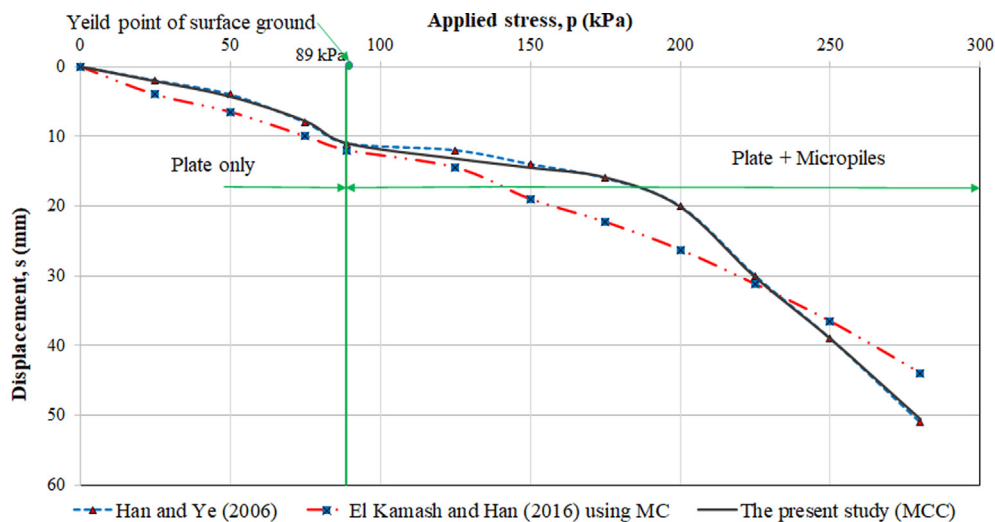


Fig. 3. Pressure-settlement curve of foundation with micropiles, comparing the analysis using the MCC model with a field plate load test, and with an analysis using the MC model.

nique, undrained conditions were simulated by setting fluid to “off”. The results of the analysis using the MCC model exhibited significantly greater agreement with the field test data [12] than that achieved by the analysis using the Mohr-Coulomb model [7]. The close agreement between the results of the present study and the field test results reported by Han and Ye [12] suggests that the Modified Cam Clay model is more appropriate than the Mohr-Coulomb model for simulating the behavior of soft clay. In Fig. 3, it can be seen that at 190 kPa the slope of the pressure-settlement curves for both the load test data and the analysis with the MCC model starts to decrease sharply, which is not the case for the analysis with the MC model. Fig. 3 indicates that for the plate-micropile system, the ground yielded at an applied stress of 190 kPa, which is significantly greater than the value of 89 kPa achieved when the plate was loaded without micropiles.

### 3. Discussion of the numerical analysis

Following validation of the Modified Cam Clay model in  $FLAC^{3D}$  with a coupled hydraulic-mechanical procedure, a numerical simulation was performed to study the effect of allowing time for consolidation, before imposing additional loads on the foundation. After application of an initial load of 89 kPa, consolidation for a period,  $t_1$ , was allowed prior to applying additional loads incrementally until the applied pressure,  $p$ , reached 280 kPa. To simulate undrained conditions, fluid was set to “off” in the  $FLAC^{3D}$  software. A staged procedure is a commonly used approach for reducing the settlement of structures over normally consolidated clay. In this study, the numerical model was used to investigate four different scenarios for loading the plate-micropile system. These scenarios are referred to as cases I to IV. The objective was

to investigate the long-term effect of the construction phase procedure, in terms of the timing of consolidation periods. A comparison of cases I and III and cases II and IV examined the effect of implementing a consolidation period before or after attaching micropiles to the foundation. In addition, a comparison of cases I and II and cases III and IV investigated the effect of preinstalling micropiles to reinforce the clay soil, prior to attaching the micropiles to the foundation.

Case I: Prior to the application of any loading stress, four bored micropiles were installed under the loading plate. The loading plate was divided into four parts, with a hole located in the center of each of the four parts. Each micropile was positioned directly beneath a hole in the plate. The holes were larger than the diameter of the micropiles, to ensure that there was initially no connection between the plate and the micropiles. Thus, the four micropiles served simply to reinforce the clay soil. The load applied to the plate was then increased from 0 kPa to 89 kPa, with fluid set to "off" in the FLAC<sup>3D</sup> software to simulate undrained conditions. Following settlement of the plate under undrained conditions at a pressure of 89 kPa, fluid was set to "on" to simulate drained conditions. The system was then allowed to settle under drained conditions for an initial consolidation period,  $t_1$ . Three values were used for  $t_1$ : 0 months (i.e., no initial consolidation period), 6 months, and 5 years. Following the consolidation period, fluid was again set to "off", simulating undrained conditions, while the micropiles were fully connected to the plate. The vertical pressure on the plate was then increased incrementally under undrained conditions, from 89 kPa to 125 kPa, then to 200 kPa, and finally to 280 kPa, and the settlement was determined for each of these pressure increments. At the final pressure of 280 kPa, drained conditions were simulated by setting fluid to "on", and a second consolidation period,  $t_2$ , was implemented, such that  $t_2 = (5 \text{ years} - t_1)$ .

Case II: The plate was placed on natural ground without micropiles and was then loaded to 89 kPa under undrained conditions, with fluid set to "off". The system was then allowed to settle under drained conditions by setting fluid to "on", for an initial consolidation period,  $t_1$ . Following the consolidation period, fluid was again set to "off", while micropiles were installed to underpin the plate, with a full connection between the micropiles and the plate. The vertical pressure on the plate was then increased incrementally under undrained conditions, from 89 kPa to 125 kPa, then to 200 kPa, and finally to 280 kPa, and the settlement was determined for each of these pressure increments. At the final pressure of 280 kPa, drained conditions were simulated by setting fluid to "on", and a second consolidation period,  $t_2$ , was implemented, such that  $t_2 = (5 \text{ years} - t_1)$ .

Case III: This case was similar to case I, where prior to loading, four bored micropiles were installed beneath holes in the plate. The holes were larger than the diameter of the micropiles, to ensure that there was initially no connection between the plate and the micropiles. Thus, the four micropiles served simply to reinforce the clay soil. The load applied to the plate was then increased from 0 kPa to 89 kPa, with fluid set to "off" to simulate undrained conditions. Following settlement of the plate under undrained conditions at a pressure of 89 kPa, the micropiles were fully connected to the plate. Fluid was then set to "on" and the system was allowed to settle under drained conditions for a consolidation period,  $t_1$ . Thus, whereas in case I the consolidation period,  $t_1$ , was implemented prior to connecting the micropiles to the plate; in case III the consolidation period was implemented after connecting the micropiles to the plate. Following consolidation under drained conditions, fluid was again set to "off" and the vertical pressure on the plate was increased incrementally under undrained conditions, from 89 kPa to 125 kPa, then to 200 kPa, and finally to 280 kPa, and the settlement was determined for each of these pressure increments. At the final pressure of 280 kPa, drained conditions

were simulated by setting fluid to "on", and a second consolidation period,  $t_2$ , was implemented, such that  $t_2 = (5 \text{ years} - t_1)$ .

Case IV: This case was similar to case II, where the plate was initially placed on natural ground without micropiles. The plate was loaded to 89 kPa under undrained conditions, with fluid set to "off", then the micropiles were installed to underpin the plate, with a full connection between the micropiles and the plate. The system was then allowed to settle under drained conditions by setting fluid to "on", for a consolidation period,  $t_1$ . Following consolidation under drained conditions, fluid was again set to "off" and the vertical pressure on the plate was increased incrementally under undrained conditions, from 89 kPa to 125 kPa, then to 200 kPa, and finally to 280 kPa, and the settlement was monitored for each of these pressure increments. At the final pressure of 280 kPa, drained conditions were simulated by setting fluid to "on", and a second consolidation period,  $t_2$ , was implemented, such that  $t_2 = (5 \text{ years} - t_1)$ .

In all four cases, the initial consolidation period,  $t_1$ , was implemented after applying the initial load of 89 kPa and before adding additional loads. A second consolidation period,  $t_2$ , was implemented after applying the final load, 280 kPa. The total consolidation time,  $t$ , remained constant, where  $t = (t_1 + t_2) = 5 \text{ years}$ . In cases I and II, micropiles were not connected to the plate until after the first consolidation period; thus, during the initial consolidation period,  $t_1$ , at 89 kPa, the plates settled alone, without micropiles. In case I, the clay soil was reinforced with micropiles during the initial consolidation period; however, in case II, there were no micropiles in the soil during this period. In cases III and IV, micropiles were connected to the plate prior to the initial consolidation period,  $t_1$ ; thus, the plate-micropile system settled as a unit during this consolidation period. It should be noted that in case III, the clay soil was reinforced with micropiles when the initial pressure of 89 kPa was applied; however, in case IV, the clay was not reinforced with micropiles at this stage.

### 3.1. Settlement

The loading of a square plate measuring 1.5 m  $\times$  1.5 m, underpinned by four micropiles in soft clay, with soil properties as shown in Table 1, was simulated numerically by using a Modified Cam Clay constitutive model. The plate was subjected to a pressure of 89 kPa and allowed to settle on the basis of consolidation of the underlying clay. This was designed to represent a shallow foundation with consolidation settlement under existing building loads. To represent additional loads on the foundation as more storeys were added to the building, the vertical pressure on the plate was increased from 89 kPa to 125 kPa, then to 200 kPa, and finally to 280 kPa. To examine the long-term effects of different consolidation periods, four different scenarios, referred to as cases I to IV, were used.

Fig. 4 shows pressure-settlement curves for cases I to IV with initial consolidation periods,  $t_1$ , of 0 months, 6 months, and 5 years. In case I, the clay was stiffer, since it was reinforced by micropiles not connected to the plate. Thus, settlement at 89 kPa was less in case I than in case II. For cases I and II, Fig. 4a and 4b suggest that allowing a consolidation period of six months or more at 89 kPa resulted in less undrained settlement of the piled raft during the load increase from 89 kPa to 280 kPa. In case I (Fig. 4a), the total settlement over a five-year period was 1157 mm, 1142 mm and 1138 mm, respectively, for a  $t_1$  of 0 months, 6 months, and 60 months, amounting to an insignificant difference. In case II (Fig. 4b), the settlement figures were slightly greater, at 1171 mm, 1190 mm and 1327 mm. In case II, a consolidation period of 60 months at 89 kPa before installation of the micropiles resulted in the greatest settlement. In case I, the micropiles prein-

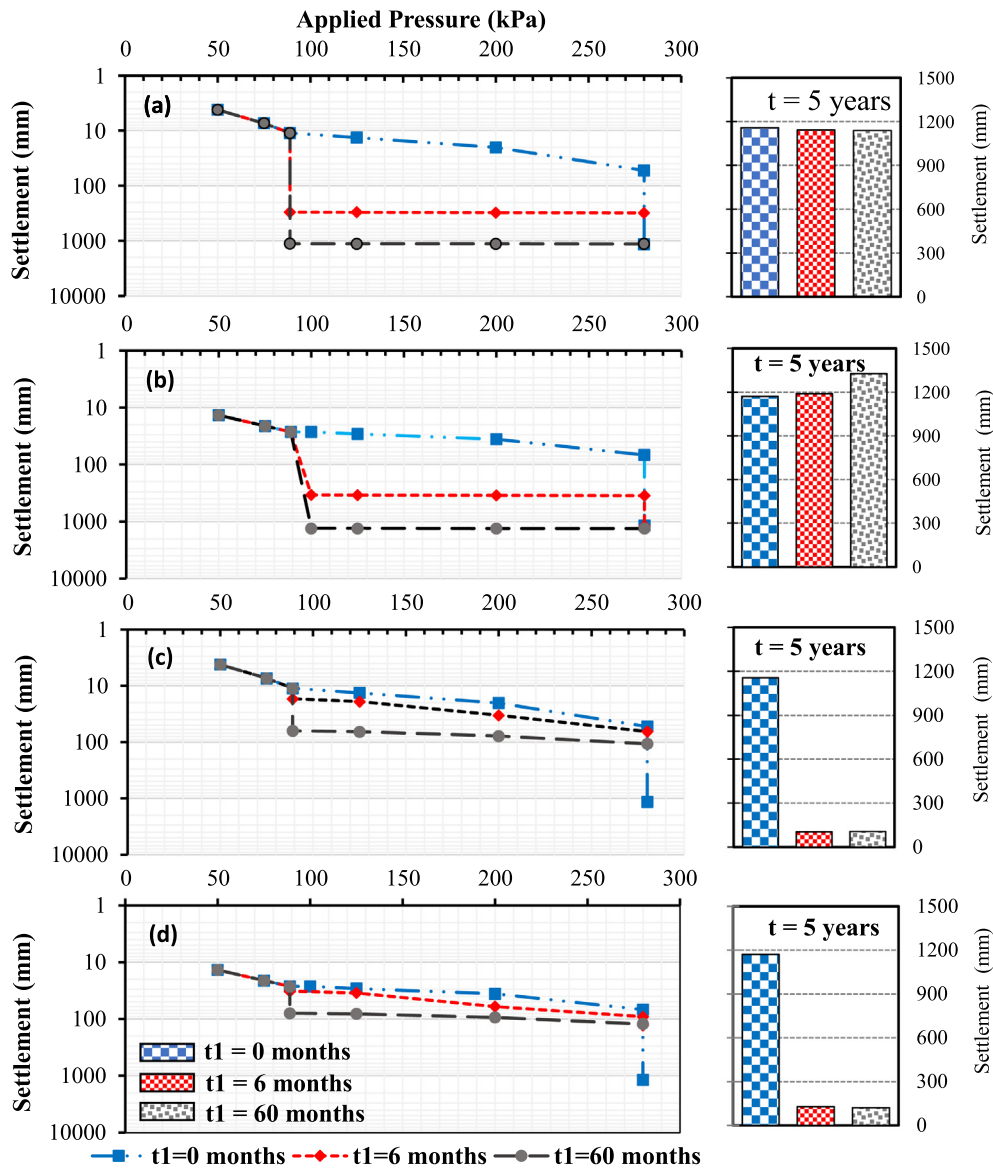


Fig. 4. Pressure-settlement curves with consolidation periods,  $t_1$ , of 0 months, 6 months, and 60 months: (a) Case I, (b) case II, (c) case III, and (d) case IV.

stalled in the clay served to reinforce the clay soil, resulting in less settlement.

In cases III (Fig. 4c) and IV (Fig. 4d), where the micropiles were connected to the plate prior to consolidation, when the initial consolidation period,  $t_1$ , was more than six months, the total settlement over a five-year period was less than 107 mm and 123 mm, respectively. However, for a  $t_1$  of 0 months, where no consolidation was permitted at 89 kPa, the total settlement over a five-year period was significantly greater, between 1171 mm and 1157 mm.

In cases III and IV, where the micropiles were connected to the plate prior to consolidation, the entire plate-micropile system settled as a unit during the initial consolidation period,  $t_1$ . This allowed for the development of mechanical and hydraulic consolidation. As shown in Fig. 4c and 4d, for both  $t_1 = 6$  months and  $t_1 = 5$  years, the total settlement was less than 107 mm for case III, and not more than 129 mm for case IV. It can be concluded that the early connection between the micropiles and the plate immediately after the application of the initial load was the most effective approach to control settlement. In both cases III and IV, there was a limited long-term settlement of around 125 mm. This is

attributable to the fact that the system could resist consolidation settlement as a single plate-micropile unit. In cases where no micropiles were connected to the plate at 89 kPa when the yield stress of the soil was reached, much greater settlement resulted.

### 3.2. Stress concentration ratio

The stress concentration ratio,  $n$ , can be defined as the ratio of the average stress on the micropiles to the average stress on the soil surrounding the micropiles below the plate, as described by El Kamash and Han [8]. The virtual Stress sensors were embedded in the numerical model to record vertical stresses at a depth of 25 cm below the plate's bottom level. The stress concentration ratio was calculated by dividing the average stresses of the micropiles by the average vertical stress of the surrounding soil at the same level.

In case I, the micropiles served to reinforce the clay, with no connection to the plate until after the consolidation period,  $t_1$ , at the applied pressure,  $p$ , of 89 kPa. In Fig. 5a it can be seen that with an increase in the applied pressure,  $p$ , indicated on the x-axis, the stress concentration ratio,  $n$ , increased significantly,

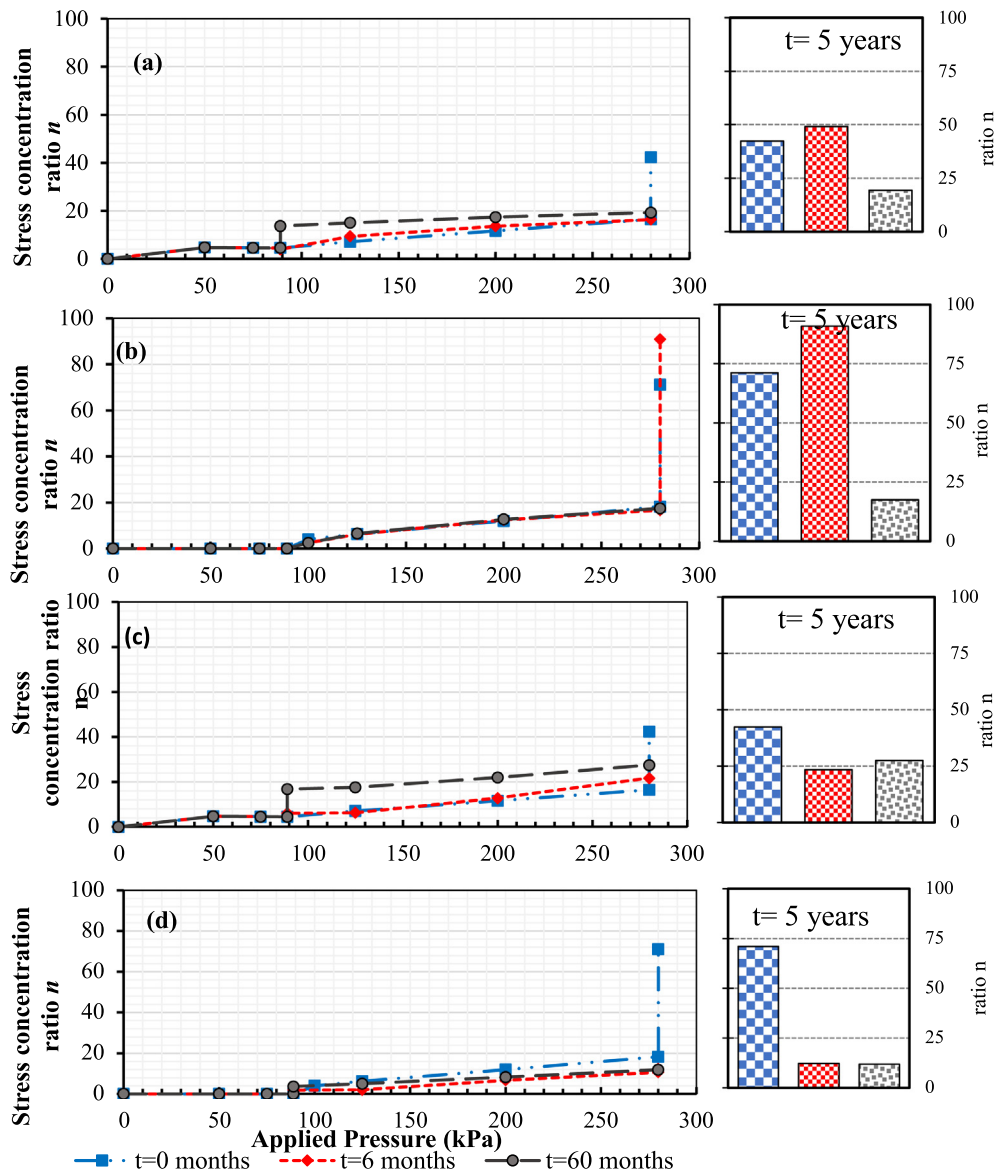


Fig. 5. Effect of the consolidation period,  $t_1$ , on the pressure-stress concentration ratio curves: (a) Case I, (b) case II, (c) case III, and (d) case IV.

depending upon the initial consolidation period,  $t_1$ . At an applied pressure of 89 kPa, the stress ratio,  $n$ , was 4.5 for a  $t_1$  of 0 months; as compared to 14 for a  $t_1$  of 60 months. This difference in the value of  $n$  can be attributed to consolidation, which takes place in the presence of the preinstalled micropiles, which are subject to stress in the form of shear stress, without being connected to the plate. At a load of 280 kPa, before implementation of the second consolidation period,  $t_2$ , (such that  $t_2 = 5 \text{ years} - t_1$ ) the stress ratio,  $n$ , was 19.26 for a  $t_1$  of 60 months, as compared to 16.38 for a  $t_1$  of 0 months.

After implementation of the second consolidation period,  $t_2$ , the value of  $n$  increased to 42.2 for the scenario where there was no initial consolidation period. This was 2.2 times greater than the value of  $n$  where the initial consolidation period,  $t_1$ , was 60 months. Thus, the stress ratio,  $n$ , was the lowest when the initial consolidation period was the longest. For cases III and IV, the implementation of the first consolidation period after the plate was connected to the micropiles enabled the micropiles to bear more of the stress directly during the consolidation process, resulting in an increase in the stress concentration ratio,  $n$ .

In case II, the micropiles were installed and connected to the plate only at the end of the first consolidation period, with a pressure of 89 kPa applied to the plate. Fig. 5b shows that the consolidation period had a slight impact on the stress concentration factor when the pressure on the plate increased from 89 kPa to 280 kPa under undrained conditions. This indicates significantly less load transfer from the surrounding soil to the micropiles. The stress concentration ratio,  $n$ , was 17.5 at  $p = 280 \text{ kPa}$  prior to the implementation of  $t_2$ , for a  $t_1$  of 0 months, 6 months, and 60 months. Following the second consolidation period,  $t_2$ , the value of  $n$  increased dramatically to 91, for a  $t_1$  of 0 months and 6 months. It can be seen that for consolidation periods,  $t_1$ , of 0 months and 6 months, the maximum values of  $n$  were much higher in case II than in case I. This was due to the reinforcement of the clay by the unconnected micropiles in the initial loading stage of case I.

In case III, the micropiles were installed and attached to the plate prior to the beginning of the first consolidation period with an applied pressure of 89 kPa on the plate. Fig. 5c shows that at 89 kPa, the value of  $n$  increased significantly, from 4.5 to 16.81, for a consolidation period,  $t_1$ , of 60 months, although the sudden

increase was much less for a  $t_1$  of 6 months. It is clear that the implementation of the initial consolidation period,  $t_1$ , after connection of the plate to the micropiles, was the primary reason for the increase in the stress ratio,  $n$ . The final stress ratio,  $n$ , following the second consolidation period,  $t_2$ , at  $p = 280$  kPa, was 28. In contrast to case I, in case III the early connection of the plate to the micropiles helped to spread the stress between the micropiles and the plate, and thus assisted in controlling the settlement.

Case IV is identical to case II, except that in case IV the micropiles were installed at  $p = 89$  kPa prior to the implementation of the first consolidation period. Fig. 5d shows that, as in case II, the initial consolidation period,  $t_1$ , did not have a significant effect on the stress ratio. However, the final values of the stress ratio,  $n$ , following the second consolidation period at 280 kPa were not more than 12, which was lower than the values in cases II and III. The fact that the maximum value of  $n$  was greater in case III than in case IV is attributable to the fact that in case III micropiles reinforced the clay during the initial loading stage, without being connected to the plate; thus, the micropiles were subject to stress in the form of shear stress.

### 3.3. Pore water pressure

Fig. 6 plots the pore water pressure,  $pp$ , 0.4 m below the center of the plate, against the applied pressure,  $p$ , in cases I, II, III, and IV for three different values of  $t_1$ . For an initial consolidation period,  $t_1$ , of 0 months, in cases I and II, the slope of the curve is slightly greater up to an applied pressure of 89 kPa, representing loads attributable to the existing building, with a very slight difference between the two cases. At 89 kPa, when the connection was made between the plate and the micropiles, a large load was transferred to the micropiles, while the load transferred to the clay was reduced. When the pressure  $p$  applied to the plate was increased from 0 kPa to 89 kPa, the pore water pressure increased rapidly from 4 kPa to 255 kPa. However, when  $p$  was increased from 89 kPa to 280 kPa, the pore water pressure increased only by 95 kPa, with the micropiles bearing most of the applied load. When a consolidation period of six months or five years was implemented at 89 kPa and additional loads were subsequently added, the pore water pressure then suddenly increased. This increase can be explained on the basis of a three-dimensional, rather than a one-dimensional, consolidation theory. As the pore water pressure moves in three dimensions, it can spread horizontally. In addition, a consolidation period,  $t_1$ , was implemented at  $p = 89$  kPa, which was determined to be the soil yield stress. The inability of the soil to withstand the consolidation settlement resulted in a rise in pore water pressure. Nevertheless, at  $p = 280$  kPa, with the plate-micropile system operating as a unit, the pore water pressure,  $pp$ , decreased from 347 kPa to 312 kPa, and from 355 to 318 kPa for cases I and II, respectively, as shown in Fig. 6a and 6b. In cases III and IV, the plate-micropile system functioned as a unit during both the first consolidation period, at 89 kPa, and the second consolidation period, at 280 kPa; the reduction of  $pp$  is shown in Fig. 6c and 6d.

In case III, the  $pp$  decreased from 256 kPa to 208 kPa at an applied pressure of 89 kPa during an initial consolidation period of 6 months; and decreased to 57 kPa during a consolidation period of 5 years, as shown in Fig. 6c. This scenario was replicated in case IV, as shown in Fig. 6d. This may reflect the significant impact of the plate-micropile system on the consolidation process, resulting in an increase in the applied pressure at which the ground yielded, from 89 kPa to 280 kPa. As shown in Fig. 6a and 6b, in cases I and II, during additional loading under undrained conditions from 89 kPa to 280 kPa, for consolidation periods,  $t_1$ , of 6 months and five years, there was a small rise in pore water pressure from 256 kPa to 346 kPa, and from 256 kPa to 311 kPa, respectively. Only for a  $t_1$

of 0 months, where no consolidation was implemented at 89 kPa, was there a noticeable increase in the pore water pressure during the application of additional loading. This is attributable to additional loads being borne primarily by the micropiles. After implementation of the second consolidation period,  $t_2$ , at  $p = 280$  kPa, the pore water pressure was 314 kPa for case I and 316 kPa for case II, regardless of the value of  $t_1$ , as shown in Fig. 6a and 6b, respectively. For cases I and II, throughout the consolidation process, the pore water pressure increased both during the first consolidation period,  $t_1$ , at 89 kPa, and the second consolidation period,  $t_2$ , at 280 kPa.

For cases III and IV, there was a significant decrease in the pore water pressure during additional loading under undrained conditions from 89 kPa to 280 kPa for a consolidation period,  $t_1$ , of 6 months, but this did not occur for a  $t_1$  of 5 years. In case III, for a  $t_1$  of 0 months, with no consolidation implemented at 89 kPa, there was a significant increase in the pore water pressure during the application of additional loading. In cases III and IV, following the implementation of the second consolidation period,  $t_2$ , at  $p = 280$  kPa, the final value of  $pp$  was 314 kPa for a  $t_1$  of 0 months, i.e., no initial consolidation period was implemented. In contrast, with an initial consolidation period,  $t_1$ , of 6 months, the final  $pp$  values were 30 kPa and 48 kPa, for cases III and IV, respectively. This underlines the substantial impact of the initial consolidation period.

### 3.4. Percentage load on the micropiles

The load on the four micropiles is comprised of the shaft and tip loads. The percentage load on the micropiles is expressed as the ratio of the micropile load at the plate level to the total load on both the micropiles and the plate. However, the percentage skin friction load on the micropiles was calculated as a percentage of the total friction and end bearing loads of all micropiles to the total applied load on the plate. In other words, it is the percentage of loads transferred by micropiles as a ratio of total applied loads. It can be calculated in the field by installing a stress gauge in the micropiles at a depth of 25 cm below the bottom level of the foundation plate. In Fig. 7a it can be seen that the initial consolidation period,  $t_1$ , implemented at the applied pressure  $p = 89$  kPa, at which the soil yielded, had a significant impact on the percentage load on the micropiles in case I. However, as shown in Fig. 7b, this did not occur in case II, since in case II no micropiles were present in the soil during the initial consolidation period. Fig. 7a shows that the load on the micropiles increased from 0% to 37% when the applied pressure was increased from 0 kPa to 89 kPa.

It should be emphasized that in case I at this stage the micropiles were installed in the clay soil, but were not connected to the plate. Thus, at this stage, loads were transferred from the plate to the micropiles in the form of shear stress. In Fig. 7a, the percentage loads of 40% and 63% at 89 kPa, for initial consolidation periods of 6 months and 5 years, respectively, can be attributed to settlement in the soft soil. This large settlement, due to the consolidation process at  $p = 89$  kPa, resulted in the transfer of loads from the soil to the micropiles.

These percentage load increases at a constant applied pressure are attributable to the weight of the soil during the consolidation process; this load was transferred to the micropiles by friction, since the yield stress of the clay soil was 89 kPa, as shown in Fig. 7a. For additional loading, to 280 kPa, the stiffness of the clay soil was enhanced due to two factors. The first factor was the consolidation period at 89 kPa, where the reduction in soil volume resulted in an increase in the bulk modulus of the soil. The second factor was the connection between the micropiles and the plate, causing the system to act as a piled raft, thus reinforcing the clay more effectively. This resulted in a decrease in the slope of the



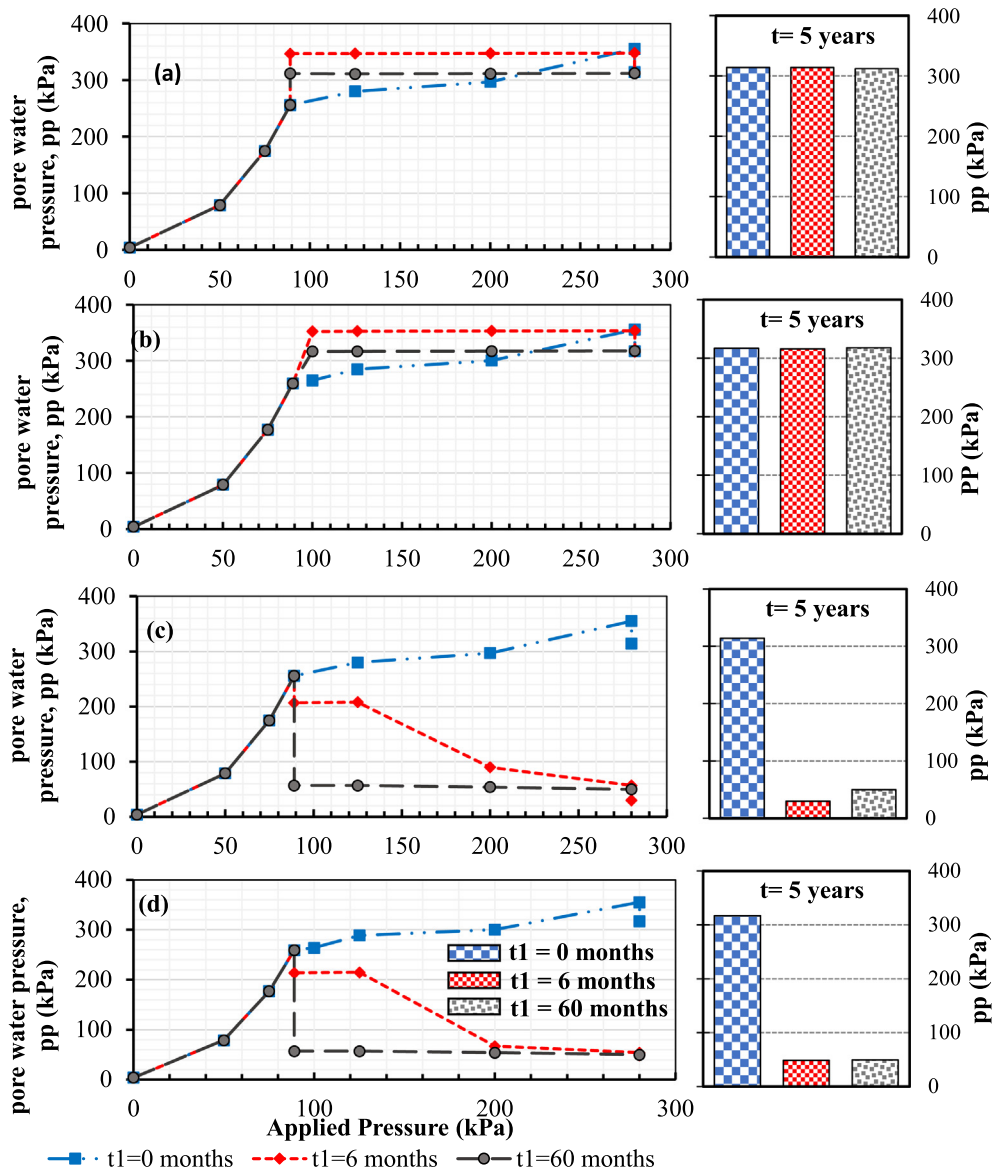


Fig. 6. Effect of the consolidation period,  $t_1$ , on the applied pressure-pore water pressure curves: (a) Case I, (b) case II, (c) case III, and (d) case IV.

pressure-percentage load curve, from an applied pressure of 89 kPa to 280 kPa, in the case of longer initial consolidation periods. Representing the clay as a Modified Cam Clay material makes it possible to allow for an increase in the bulk modulus of the clay soil as a result of the consolidation process.

- In case I, for an initial consolidation period,  $t_1$ , of 5 years, with an increase in  $p$  from 89 kPa to 280 kPa, the percentage load on the micropiles increased from 63% to 71%, with a slope of 0.04. As shown in Fig. 7a, for initial consolidation periods of 0 months and 6 months, the slope of the curve was not less than 0.14.
- In case II (Fig. 7b), no micropiles were present in the soil when  $p$  was increased from 0 kPa to 89 kPa. The micropiles were installed and the foundation began to operate as a micropile-plate system only after the initial consolidation period at 89 kPa had been completed. As a result, the initial consolidation period did not affect the percentage load on the micropiles. Thus, in case II the percentage load was zero as  $p$  increased from 0 kPa to 89 kPa. However, as  $p$  increased from 89 kPa to 280 kPa, the percentage load increased from 0% to 70%, with a slope of

0.37. In case I, as shown in Fig. 7a, at  $p = 280$  kPa the percentage load increased from 68% to 90%, due to the implementation of a second consolidation period,  $t_2$ . Similarly, in case II, at 280 kPa the percentage load on the micropiles increased from 70% to 84%, as shown in Fig. 7b.

- The scenario of case III was the same as that of case I, except that in case III the micropiles were connected to the plate prior to the beginning of the initial consolidation period,  $t_1$ , at  $p = 89$  kPa. Thus, a  $t_1$  of 5 years resulted in a load of 68% in case III, as compared to a load of 63% in case I, as shown in Fig. 7c and 7a, respectively. At 280 kPa, with initial consolidation periods of 6 months and 5 years, the percentage load was 73% and 78%, respectively, in case III, and 70% in case I. This improvement in the percentage load in case III, relative to case I, was due to the fact that in case III the micropiles and the plate were connected prior to the initial consolidation period at 89 kPa.
- In contrast to case II, in case IV the initial consolidation period,  $t_1$ , had a significant effect on the percentage load, with a longer consolidation period resulting in a higher percentage load, as shown in Fig. 7d. For initial consolidation periods of 6 months

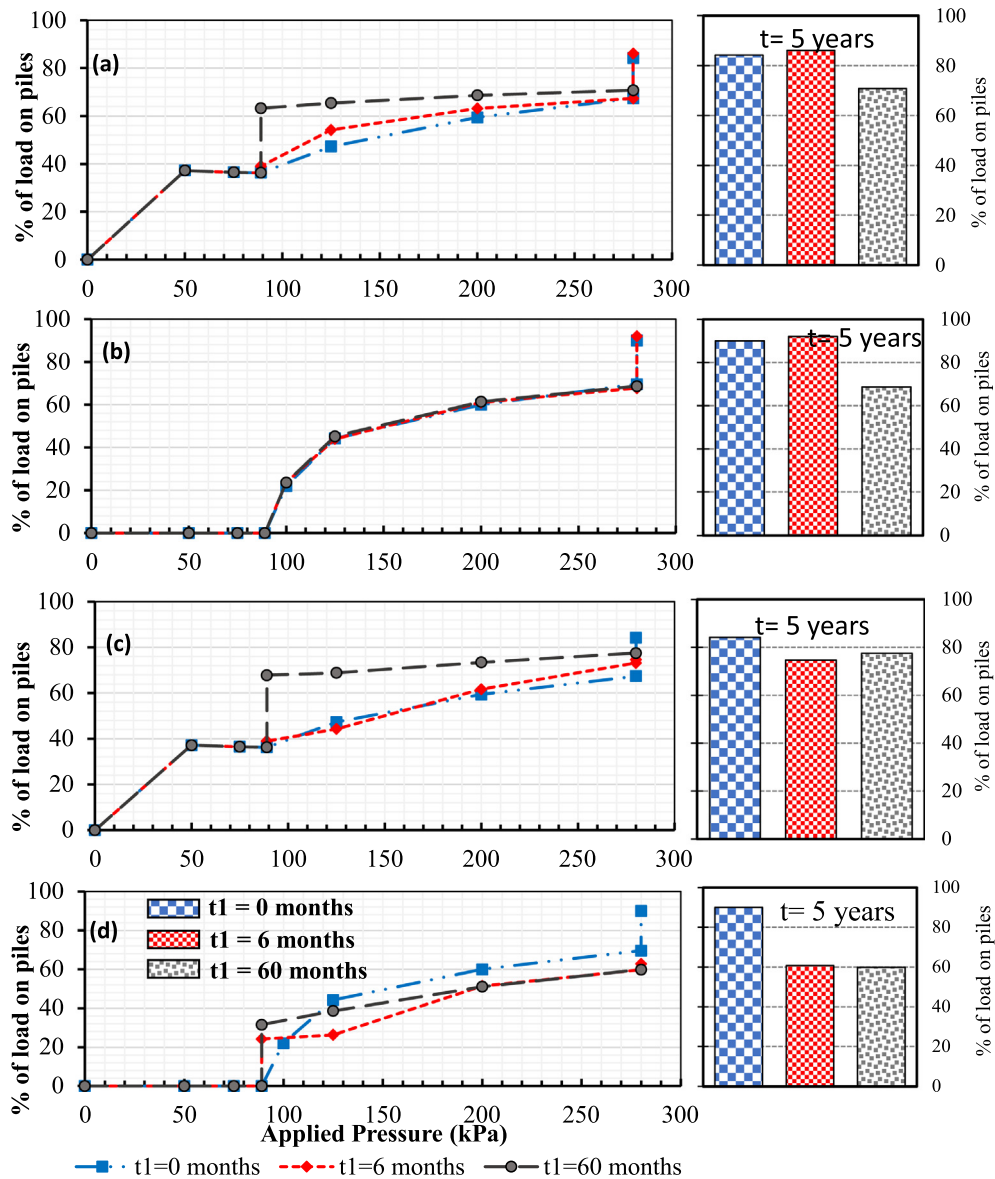


Fig. 7. Effect of the consolidation period,  $t_1$ , on the percentage load on the micropiles: (a) Case I, (b) case II, (c) case III, and (d) case IV.

and 5 years, the percentage load at  $p = 89$  kPa was 25% and 32%, respectively. As shown in Fig. 7d, as  $p$  increased from 89 kPa to 280 kPa, the slope of the pressure-percentage load curve was steeper for a  $t_1$  of 0 months than for a  $t_1$  of 5 years. However, at  $p = 280$  kPa, as a result of the implementation of a second consolidation period,  $t_2$ , the percentage load increased from 63% to 90% for a  $t_1$  of 0 months and 6 months.

At  $p = 280$  kPa, prior to the implementation of a second consolidation period,  $t_2$ , it can be seen that a longer initial consolidation period contributed to a higher percentage load in case III, whereas this did not occur in case IV. This may be attributable to the fact that in case III, the preinstalled micropiles that were not connected to the plate were nevertheless subject to stress during the application of pressure from 0 kPa to 89 kPa. In contrast, this did not happen in case IV since no micropiles were installed at that stage. It can be concluded that the early preinstallation of micropiles resulted in a significant increase in the contribution of the micropiles to support the loads applied to the plate.

### 3.5. Skin friction

Skin friction along micropile can be calculated on the basis of  $\tau_z = (\sigma_{zz}^{i+1} - \sigma_{zz}^i - \sigma_w^i) A_p / A_s$ , where  $\sigma_{zz}^{i+1}$  and  $\sigma_{zz}^i$  are the axial stresses in the micropiles at node  $i + 1$  (node  $i + 1$  was above node  $i$ ),  $-\sigma_w^i$  is the self weight of the element  $j$  between  $i$  and  $i + 1$ ,  $A_p$  is the cross sectional area of the micropile, and  $A_s$  is the surface of the micropiles between nodes  $i$  and  $i + 1$ . The depth distribution of the skin friction along the micropiles at the maximum applied pressure,  $p = 280$  kPa, following implementation of the second consolidation period,  $t_2$ , can be plotted as shown in Fig. 8. It should be noted that a positive skin friction indicates that the amount of normal stress at the top of the micropile and the weight of the section itself exceeds the normal stress at the bottom of the micropile, which means that the friction between the micropile and the soil helps to support the micropile. In contrast, a negative skin friction generally means that the micropile segment is affected by a downward shear drag, due to downward movement of the soil relative to the micropile.

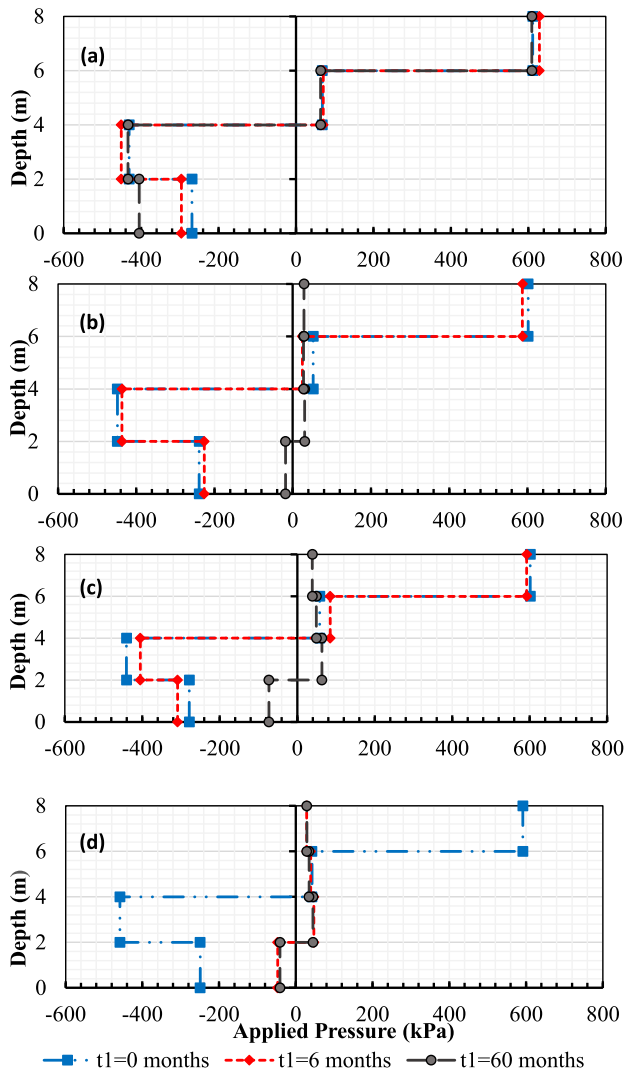


Fig. 8. Effect of consolidation period,  $t_1$ , on skin friction distribution along the micropiles at maximum applied pressure,  $p = 280$  kPa: (a) Case I, (b) case II, (c) case III, and (d) case IV.

Fig. 8a shows that in case I, the initial consolidation period,  $t_1$ , affected the skin friction in the top 2 m of the micropile, with skin friction values of  $-268$ ,  $-269$ , and  $-400$  kPa corresponding to  $t_1$  of 0 months, 6 months, and 60 months, respectively. At a depth of 2 to 4 m, the skin friction was approximately  $-450$  kPa, regardless of the initial consolidation period. The skin friction was approximately  $64$  kPa at a depth of 4 to 6 m, and  $620$  kPa at a depth of 6 to 8 m.

It can be seen that the skin friction increased with depth for cases I and II. The initial consolidation period had a more noticeable effect on the skin friction in the upper part of the micropile, and the effect was less apparent at greater depths, as shown in Fig. 8a and b. At a depth of 4 m, a skin friction value of up to  $14$  kPa was found for both cases I and II, as shown in Fig. 8a and 8b. In case II, for an initial consolidation period of 60 months, skin friction values were relatively low, ranging from  $-18$  kPa to  $31$  kPa, as can be seen in Fig. 8b. This is due to the fact that in case II, no micropiles were present when the applied stress,  $p$ , was increased from  $0$  kPa to  $89$  kPa. In contrast, in case I, the preinstalled micropiles that were not yet connected to the plate nevertheless contributed to the skin friction. For an initial consolidation period of 60 months at  $p = 89$  kPa, the micropiles were subject to friction stress in the form of shear stress.

As shown in Fig. 8c, the skin friction values in case III were similar to those in case I, except that for an initial consolidation period of 60 months, the range of skin friction values from the top to the bottom of the micropile was  $-71$  kPa to  $38$  kPa in case III, a much smaller range than that found in case I. This difference is due to the fact that in case III the micropiles were connected to the plate prior to the initial consolidation period,  $t_1$ , at  $89$  kPa. The early connection of the micropiles to the plate to form a plate-micropile system increased the load-bearing capacity of the foundation and helped to reduce the amount of settlement.

The skin friction distribution in case IV was similar to that of the cases discussed above. For initial consolidation periods of 6 months and 60 months, the skin friction ranged from  $-41$  kPa to  $28$  kPa, and the transition from negative to positive skin friction occurred at a depth of 2 m, as shown in Fig. 8d.

Fig. 9 shows the effect of the initial consolidation period,  $t_1$ , on the percentage skin friction load on the micropiles for cases I, II, III and IV. Fig. 9a indicates that for case I, the initial consolidation period at an applied pressure of  $89$  kPa had a significant effect on the skin friction load, resulting in values of  $91\%$ ,  $76\%$ , and  $61\%$  for a  $t_1$  of 0 months, 6 months, and 60 months, respectively. These results show the effect of consolidation on decreasing the percentage skin friction load, taking end bearing into account. As shown in Fig. 9a, at an applied pressure,  $p$ , of  $280$  kPa, for a  $t_1$  of 60 months, the skin friction load was  $84\%$ . For a  $t_1$  of 0 months, the skin friction load at  $280$  kPa decreased from  $97\%$  to  $90\%$  during the second consolidation period,  $t_2$ . The effect of the initial consolidation period on the percentage skin friction load was due the fact that micropiles were preinstalled, without being connected to the plate, at an applied pressure representing the load of the existing building. In contrast, as shown in Fig. 9b, in case II, the initial consolidation period had no significant effect on the final skin friction load, which ranged from  $94\%$  to  $96\%$ , regardless of the consolidation period.

As shown in Fig. 9c, in case III, the initial consolidation period,  $t_1$ , affected the percentage skin friction load only in the applied pressure range of  $89$  kPa to  $125$  kPa. At an applied pressure,  $p$ , of  $89$  kPa, the skin friction load was  $91\%$ ,  $61\%$ , and  $86\%$  for a  $t_1$  of 0 months, 6 months, and 60 months, respectively. For the applied pressure range of  $125$  kPa to  $280$  kPa, the skin friction load was  $98\%$ , regardless of the initial consolidation period. In case IV, the skin friction load ranged from  $90\%$  to  $98\%$  in the applied pressure range of  $100$  kPa to  $280$  kPa, without being significantly affected by the initial consolidation period. As shown in Fig. 9d, the skin friction load at  $280$  kPa following the implementation of a second consolidation period,  $t_2$ , was  $98\%$  for a  $t_1$  of 6 months and 60 months, as compared to  $91\%$  for a  $t_1$  of 0 months.

#### 4. Conclusions

Although micropiles are efficient in providing short-term stability by underpinning existing foundations to carry additional loads, this approach can result in large consolidation settlements in the long term. Few studies have been done so far to investigate the effects of consolidation on the behavior of foundations underpinned by micropiles in soft clay. In the current study, a 3D coupled hydraulic-mechanical analysis was performed based on a hardening MCC constitutive soil model, to examine the effects of consolidation on the stability of foundations underpinned by micropiles. The innovative numerical model using the MCC approach was verified with field tests and plate loading tests performed on natural ground. A parametric study was carried out to examine the effects of implementing a consolidation period prior to the application of additional loading. The current study was developed based on verified models for different micropile instal-

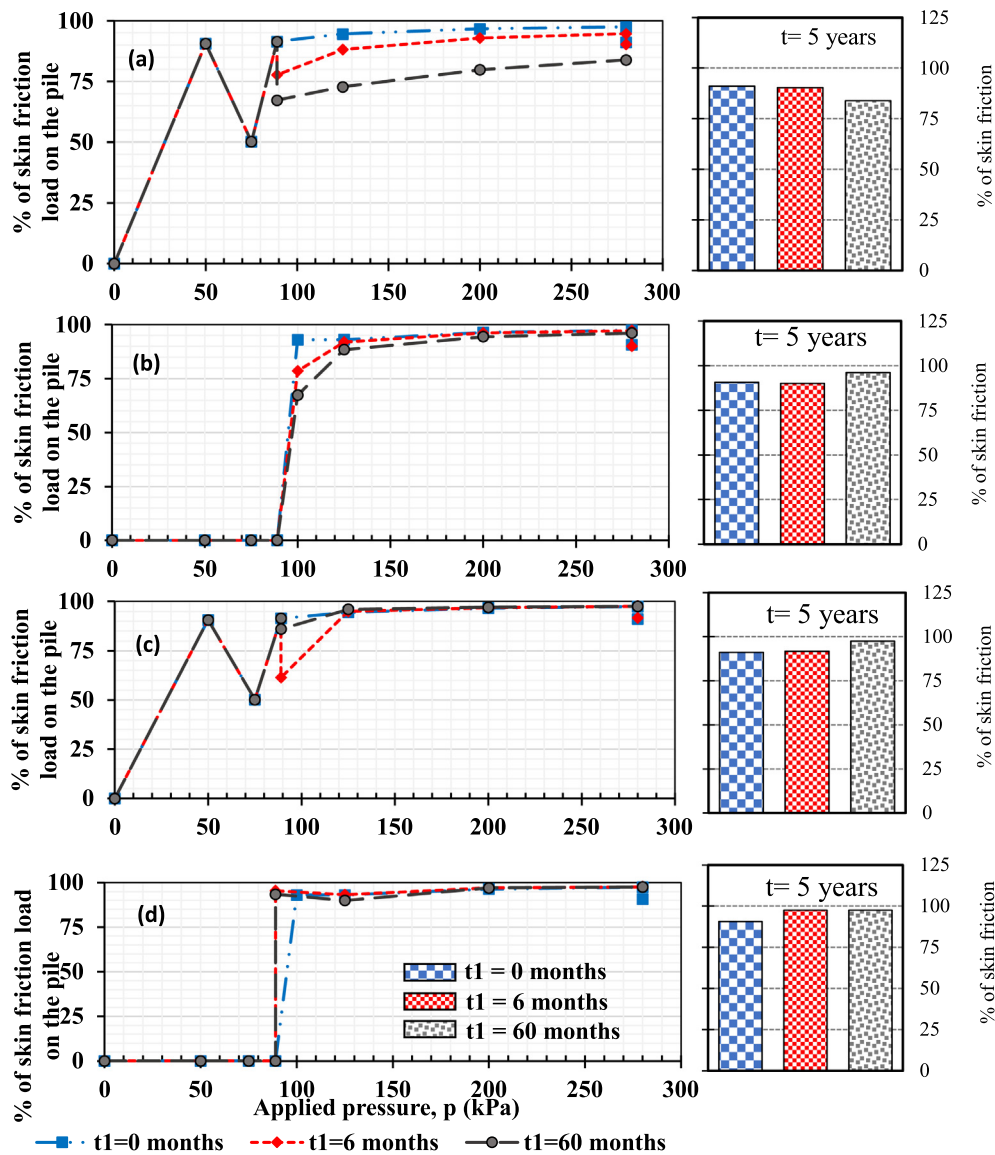


Fig. 9. Effect of the consolidation period,  $t_1$ , on the percentage skin friction load on the micropiles: (a) Case I, (b) case II, (c) case III, and (d) case IV.

lation procedures. The numerical study resulted in the following conclusions, according to the circumstances in which the floating micropiles were installed in soft clay.

- For the simulation of a consolidation process where a reduction in soil volume results in an increase in the bulk modulus of the soil, the Modified Cam Clay constitutive model was found to yield more accurate results than the conventional Mohr-Coulomb model, when modeling a shallow foundation underpinned by micropiles in soft clay.
- Studying the behavior of foundations underpinned by micropiles only in undrained conditions (short-term settlement) does not permit a comprehensive understanding of the foundation behavior. Thus, the coupled hydraulic-mechanical numerical model using the MCC approach, for both drained and undrained conditions, was found to be more accurate for investigating the long-term behavior of foundations on soft clay.
- The implementation of an early consolidation period after connecting the micropiles to the plate to form a plate-micropile system was found to have a significant positive effect on controlling the settlement.

- A long consolidation time led to greater settlement of the plate and a smaller percentage skin friction load on the micropiles. As the consolidation increased, the dissipation of excess pore water pressure also increased, which served to enhance the ability of the soft clay soil to support additional loads.

These conclusions have been drawn in accordance with the four cases discussed above, where floating micropiles were installed in soft clay.

### 5. Data availability

All data, models, and code generated or used during the study appear in the submitted article.

### Declaration of Competing Interest

The authors declare that they have no known competing financial interests or personal relationships that could have appeared to influence the work reported in this paper.

## References

- [1] Alnuaim AM, El Naggar MH, El Naggar H. Performance of micropiled raft in clay subjected to vertical concentrated load: centrifuge modeling. *Can Geotech J* 2015;52(12):2017–29. doi: <https://doi.org/10.1139/cgj-2014-0001>.
- [2] Alnuaim AM, El Naggar H, El Naggar MH. Performance of micropiled raft in sand subjected to vertical concentrated load: centrifuge modeling. *Can Geotech J* 2015;52(1):33–45. doi: <https://doi.org/10.1139/cgj-2014-0001>.
- [3] Alnuaim AM, El Naggar MH, El Naggar H. Numerical investigation of the performance of micropiled rafts in sand. *Comput Geotech* 2016;77:91–105. doi: <https://doi.org/10.1016/j.compgeo.2016.04.002>.
- [4] Alnuaim AM, El Naggar MH, El Naggar H. Performance of micropiled rafts in clay: Numerical investigation. *Comput Geotech* 2018;99:42–54. doi: <https://doi.org/10.1016/j.compgeo.2018.02.020>.
- [5] Borthakur, N., & Dey, A. K. (2018). Experimental investigation on load carrying capacity of micropiles in soft clay. *Arabian Journal for Science and Engineering*, 43(4), 1969–1981. DOI: <https://doi.org/10.1007/s13369-017-2894-3>.
- [6] Capatti MC, Carbonari S, Gara F, Roia D, Dezi F. June). Experimental study on instrumented micropiles. In: *In 2016 IEEE Workshop on Environmental, Energy, and Structural Monitoring Systems (EESMS)*. IEEE; 2016. p. 1–6.
- [7] El Kamash W, Han J. Numerical analysis of existing foundations underpinned by micropiles. *Int J Geomech* 2017;17(6):04016126. doi: [https://doi.org/10.1061/\(ASCE\)GM.1943-5622.0000833](https://doi.org/10.1061/(ASCE)GM.1943-5622.0000833).
- [8] El Kamash, W., Han, J., & ASCE, F. (2014). Displacements of column-supported embankments over soft clay after widening considering soil consolidation and column layout: Numerical analysis. *Soils and Foundations*, 54(6), 1054–1069. DOI: <https://doi.org/10.1016/j.sandf.2014.11.002>.
- [9] Manual, F. U. S. (1992). Itasca Consulting Group.
- [10] FHWA, N. (2005). *Micropile design and construction—reference manual*. Federal Highway Administration–National Highway Institute (FHWA NHI). US Department of Transportation, McLean, Va. Publication No. FHWA NHI-05-039.
- [11] Guo Z, Khidri M, Deng L. Field loading tests of screw micropiles under axial cyclic and monotonic loads. *Acta Geotech* 2019;14(6):1843–56.
- [12] Han J, Ye SL. A field study on the behavior of micropiles in clay under compression or tension. *Can Geotech J* 2006;43(1):19–29.
- [13] Lizzi F, Carnevale G. Les Reseaux de pieux racines pour la consolidation des sols, aspects theoretique et essais sur mondile. *Proc. Int. Conf., Soil Reinforcement, Paris 1979*;2:317–24.
- [14] Kyung D, Kim D, Kim G, Lee J. Vertical load-carrying behavior and design models for micropiles considering foundation configuration conditions. *Can Geotech J* 2017;54(2):234–47. doi: <https://doi.org/10.1139/cgj-2015-0472>.
- [15] Mashhoud HJ, Yin JH, Panah AK, Leung YF. A 1-g shaking table investigation on response of a micropile system to earthquake excitation. *Acta Geotech* 2020;15(4):827–46. doi: <https://doi.org/10.1007/s11440-018-0742-6>.
- [16] Ni P, Song L, Mei G, Zhao Y. Generalized nonlinear softening load-transfer model for axially loaded piles. *Int J Geomech* 2017;17(8):04017019. doi: [https://doi.org/10.1061/\(ASCE\)GM.1943-5622.0000899](https://doi.org/10.1061/(ASCE)GM.1943-5622.0000899).
- [17] Qian, Z. Z., & Lu, X. L. (2011). Behavior of micropiles in soft soil under vertical loading. In *Advanced Materials Research* (Vol. 243, pp. 2143–2150). Trans Tech Publications.
- [18] Srivastava A, Kumar P, Babu GS. *Stability analyses of 18 m deep excavation using micro piles*. Delhi: IGC, N; 2016.
- [19] Seo H, Prezzi M, Salgado R. Instrumented static load test on rock-socketed micropile. *J Geotech Geoenviron Eng* 2013;139(12):2037–47. doi: [https://doi.org/10.1061/\(ASCE\)GT.1943-5606.0000946](https://doi.org/10.1061/(ASCE)GT.1943-5606.0000946).
- [20] Singh, S., & Heine, E. I. (1984). Upgrading existing footings with micro-piles.
- [21] Sharma, B., Zaheer, S., & Hussain, Z. (2014). Experimental model for studying the performance of vertical and batter micropiles. In *Geo-Congress 2014: Geo-characterization and Modeling for Sustainability* (pp. 4252–4264).
- [22] Tsukada Y, Miura K, Tsubokawa Y, Otani Y, You GL. Mechanism of bearing capacity of spread footings reinforced with micropiles. *Soils Found* 2006;46(3):367–76. doi: <https://doi.org/10.3208/sandf.46.367>.
- [23] Zhang QQ, Zhang ZM, He JY. A simplified approach for settlement analysis of single pile and pile groups considering interaction between identical piles in multilayered soils. *Comput Geotech* 2010;37(7–8):969–76. doi: <https://doi.org/10.1016/j.compgeo.2010.08.003>.
- [24] Biot. Theory of propagation of elastic waves in a fluid-saturated porous solid. II. Higher frequency range. *The Journal of the acoustical Society of America* 1956;28(2):179–91.



Dr. El Kamash is a Senior Consultant who solves problems with problematic soils and designs special foundations. He is the vice dean of the Engineering Faculty at Suez Canal University. He is an Associate Professor and accredited geotechnical and foundation consultant, with a philosophy of doctorate degree and a Master of Science degree from Suez Canal University, as well as a visiting scholar of the Faculty of Engineering at many international universities, including James Cook University in Australia and the University of Kansas in the United States. Dr. El Kamash began his career in an international oil and gas company, Belayim Petroleum Company (PETROBEL), where he held several positions before transitioning to academia as a staff member specialising in geotechnical engineering and structural design. He has taught in Egypt, Saudi Arabia, and universities in the United States. Furthermore, he provides consulting and professional training to major oil and gas companies' employees. Dr. El Kamash is a partner in the "Group of advanced consultations in geotechnical and structures; EGF," which contributes to the design and consulting of many projects, particularly in oil and gas companies like Petrobel and EPC.